Supplementary Information

Self-Nanofibrillation Strategy to Unusual Combination of Strength and Toughness for Poly(lactic acid)

Lan Xie,* *Xin Sun*, *Yaozhu Tian*, *Fuping Dong*,

Min He, *Yuzhu Xiong** and *Qiang Zheng*

Department of Polymer Materials and Engineering, College of Materials and Metallurgy, Guizhou University, Guiyang 550025, China

*Corresponding Authors: lancysmile@163.com or mm.lanxie@gzu.edu.cn (L.X.);

932271187@qq.com (Y.X.)

This Supporting Information contains 6 figures in 8 pages.

EXPERIMENTAL SECTION

Materials. Poly(lactic acid) (PLA) under a trade name of 4032D comprising ~2% $_D$-LA was purchased from NatureWorks (USA), being characterized by weight-average and number-average molecular weights of 2.23×10^5 g/mol and 1.06×10^5 g/mol, respectively. PLA was isothermally annealed at 120 °C for 30 min to obtain sufficient crystallization.

Sample Preparation. A twin screw extruder equipped with a slit die (20 mm in width and 2 mm in height) was used to produce nanofibrillar structure in pure PLA. Intensive elongational shear flow was generated in the extruder with a high ratio of screw length to diameter (L/D) of 40, with barrier temperatures set at 80, 120, 150, 165, 165, 165 and 160 °C from feed section to die, respectively. The extrudate was directly hot stretched through the slit die by a take-up device with two pinching rolls to obtain high-speed stretching, wherein the rolling speed was tuned to obtain high drawing ratios of 10 for moderately drawn PLA (MD PLA) and 20 for highly drawn PLA (HD PLA). The roll temperature was controlled at 60 °C by the flux of cooling water. The as-stretched PLA sheets were immediately quenched in a cold water bath (20 °C) to freeze the formed fibrils in the self-nanofibrillar PLA. It is worth noting that the control samples of normal PLA subjected to the drawing ratio of 1 (no stretching after extrusion) were also prepared. Particularly, three crucial processing parameters were used to produce an intensive shear and stretching flow aiming at deliberate control over the nanofibrillar textures (such as the fibril size and alignment): (1) low processing temperature close to the melting point of PLA to permit the survival of considerable amount of highly ordered PLA crystals; (2) a high ratio of screw length to diameter (L/D) of 40, enabling sufficient breakup and deformation of crystalline entities; (3) a high screw speed (250 rpm) to create an elongational shear flow in the melts with strengthened mechanical stress and shear; (4)

high-speed stretching of extrudate to suppress the retraction or disengagement of the oriented structures.

SEM Observation. SEM was employed to observe the fibrillar structure and crystalline morphology for self-nanofibrillar PLA. Cryogenic fracture and alkaline etching were applied to obtain the specific surfaces. For the cryogenic fracture, the as-stretched ribbons were placed in liquid nitrogen for 0.5 h and cryogenically fractured along the stretching direction. The fracture surfaces were directly taken or further etched for SEM observation. To observe the crystalline morphology in self-nanofibrillar PLA, amorphous PLA was etched in a water-methanol (1:2 by volume) solution containing 0.025 mol/L of sodium hydroxide for 14 hours at 15 °C. All the etched surfaces were cleaned by using distilled water with the assistance of ultrasonication. A field-emission SEM (Inspect F, FEI, Finland) was utilized to explore the fibrillar and crystalline morphology of the self-nanofibrillar PLA sputter-coated with gold, while the accelerated voltage was held at 5 kV.

Synchrotron X-Ray Measurements. Two-dimensional wide-angle X-ray diffraction (2D-WAXD) determination was carried out at the beamline BL15U1 of Shanghai Synchrotron Radiation Facility (SSRF, Shanghai, China). The monochromated X-ray beam with a wavelength of 0.124 nm was focused to an area of 3 × 2.7 μm^2 (length × width), and the sample-to-detector distance from was set as 185 mm. After 90-second exposure to the X-ray for the samples, the 2D-WAXD images were collected with an X-ray CCD detector (Model SX165, Rayonix Co. Ltd, USA).

Two-dimensional small-angle X-ray scattering (2D-SAXS) measurements were performed at the beamline BL16B1 of SSRF. The 2D-SAXS images were collected with an X-ray CCD detector (Model Mar165, a resolution of 2048 × 2048 pixels). The monochromated X-ray beam operated at a wavelength of 0.124 nm with a beam size of 80 × 80 μm^2 (length × width), and the sample-to-

detector distance was fixed at 2140 mm. The radically integrated intensities $I(q)$ ($q = 4\pi\sin\theta/\lambda$) are obtained for integration in the azimuthal angular range of a whole circle, where 2θ stands for the scattering angle and λ represents the X-ray wavelength. The long period (L) regarding the lamellar structure was calculated using the Bragg equation, $L = 2\pi/q^*$.

Differential Scanning Calorimeter (DSC). Annealed PLA prior to extrusion, normal PLA and self-nanofibrillar PLA after extrusion were heated from 25 to 200 °C on a DSC Q200 (TA Instruments, USA) at a heating rate of 10 °C/min under nitrogen atmosphere.

Tensile Property Testing. According to ASTM standard D638: 1999, the tensile properties were measured at room temperature on an Instron universal test instrument (Model 5576, Instron Instruments, USA) with a crosshead speed of 20 mm/min and a gauge length of 20 mm. A minimum of 5 bars for each sample were tested at the same conditions, and the average values were presented with standard deviation.

RESULTS AND DISCUSSION

Figure S1a shows the high melt strength of extruded PLA amenable to high-drawing-ratio stretching, due primarily to the existence of shear-aligned crystals that survived from the melting at 165 °C. The high flexibility allowed the as-stretched PLA ribbons to be woven into a mat (Figure S1b).

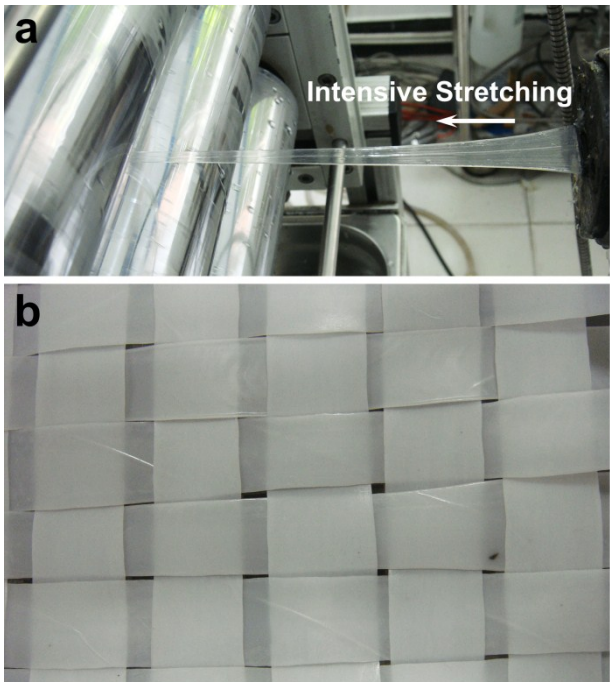

Figure S1. Digital photos showing (a) hot stretched PLA from the slit die, and (b) HD PLA sheets with high flexibility that can be easily woven into a mat.

Figure S2 shows that isothermally annealed PLA was characterized by a high degree of crystallinity (56.8%), a glass transition temperature at 42.7 °C and a melting point at 167.1 °C.

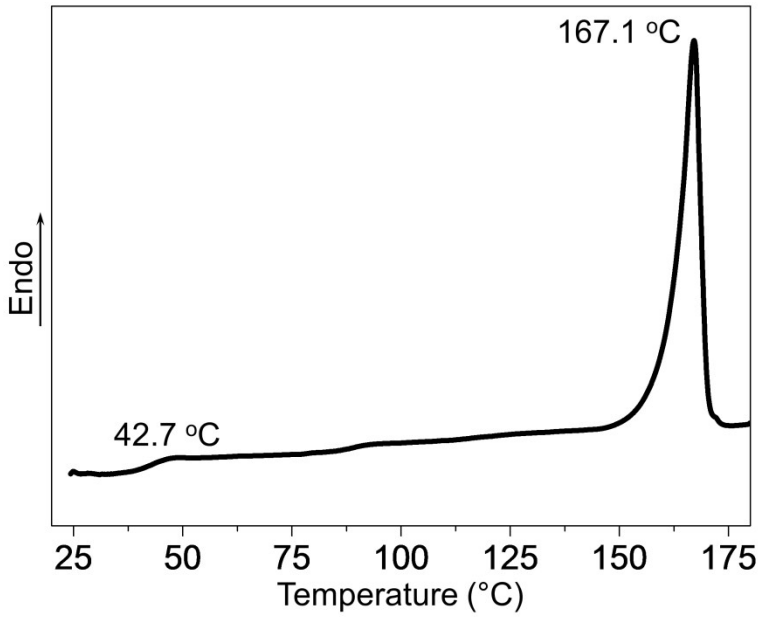

Figure S2. DSC heating curve of PLA isothermally annealed at 120 °C for 30 min.

Figure S3 shows that no traces of nanofibrillar texture or structural evolution were observed in normal PLA.

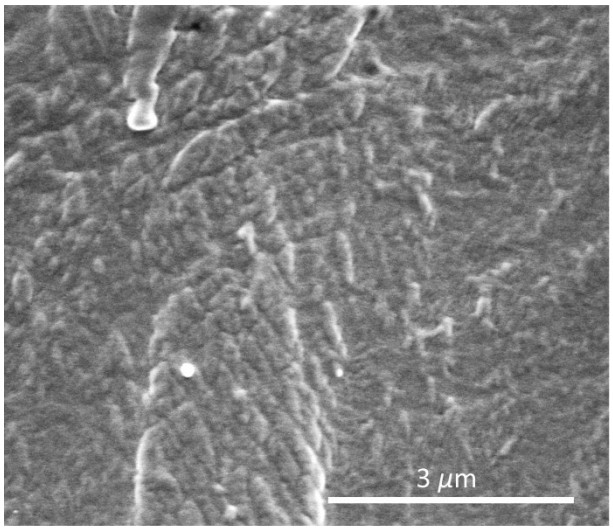

Figure S3. SEM image of cryogenic fracture surface of normal PLA.

In line with the DSC data and 2D-WAXD results, Figure S4 shows that no evident formation of crystalline entities was observed in normal PLA.

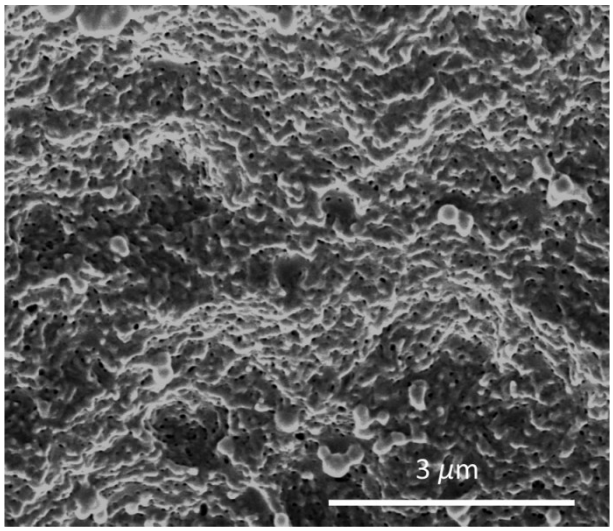

Figure S4. SEM image of normal PLA after alkaline etching.

Figure S5 shows the crystalline morphology developed in self-nanofibrillar PLA, as a complement for Figure 2a,b. It is obvious that the aligned shish was characterized by extremely high density and structural integrity for both MD PLA and HD PLA.

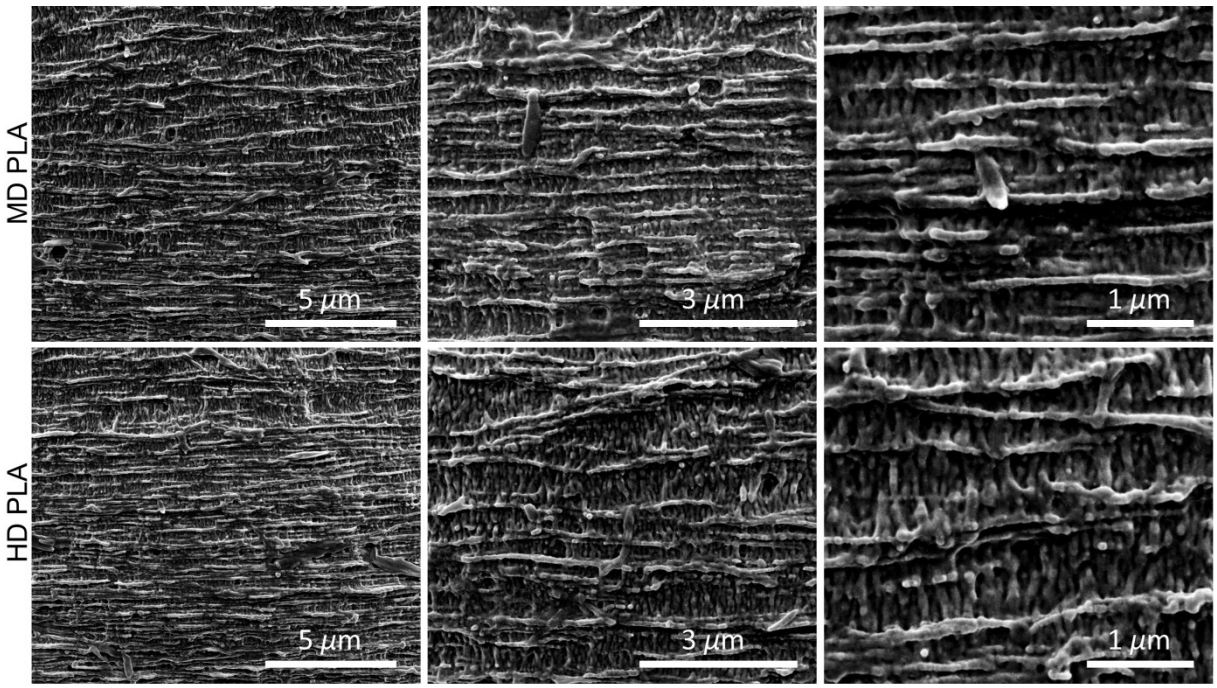

Figure S5. SEM micrographs of MD PLA and HD PLA showing the crystalline morphology.

1D-WAXD intensity profiles characterized the almost amorphous state for normal PLA, but a large amount of α-form crystals for self-nanofibrillar PLA (Figure S6). The crystallinity in MD PLA

is significantly higher than that of HD PLA, indicating the enhanced nucleation activity of PLA under the stretching flow of higher intensity.

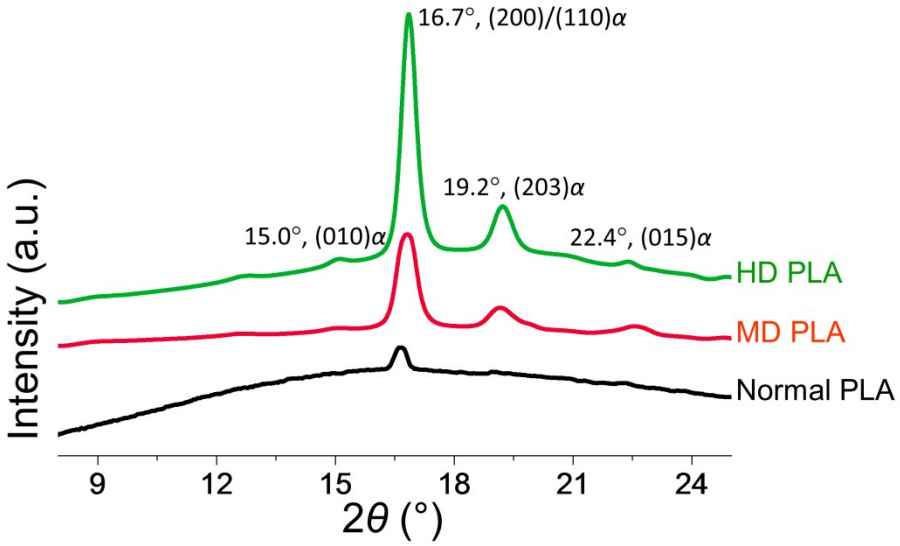

Figure S6. 1D-WAXD intensity profiles of normal PLA, MD PLA and HD PLA showing the almost amorphous state in normal PLA and dense α-form crystals developed in self-nanofibrillar PLA.

Probably due to the relatively low contents of amorphous chains in self-nanofibrillar PLA, the glass transition behavior was not as significant as normal PLA (Figure 3f, main text). Figure S7 extracts the DSC curves of MD PLA and HD PLA in the glass-transition region for direct comparison.

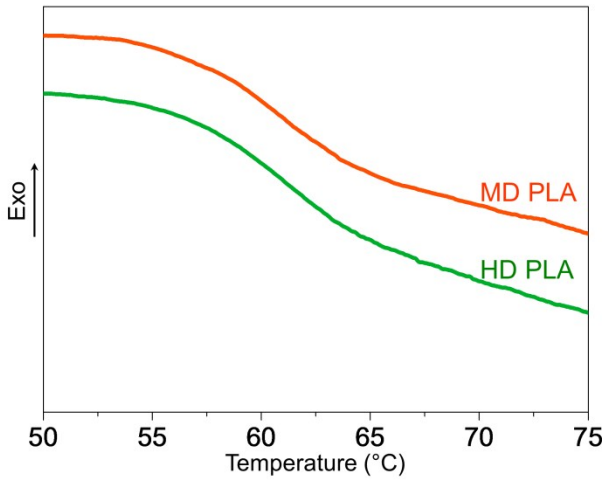

Figure S7. DSC heating curves of MD PLA and HD PLA in the glass-transition region.

Table S1 lists the detailed values of tensile properties for self-nanofibrillar PLA, as extracted from the stress−strain curves (Figure 3a, main text). The tensile toughness or the energy taken up by the PLLA/QD composites before breaking was evaluated by calculating the area under the stress−strain curve.

Table S1. Detailed Tensile Properties of Normal PLA and Self-Nanofibrillar PLA[a]

Sample	Tensile Strength (MPa)	Tensile Modulus (MPa)	Elongation at Break (%)	Toughness (MJ/m^3)[b]
Normal PLA	46.9 ± 5.7	1316 ± 124	7.8 ± 1.2	2.5 ± 0.4
MD PLA	51.4 ± 6.5	1365 ± 169	145.3 ± 11.3	42.7 ± 5.3
HD PLA	63.7 ± 3.6	2193 ± 209	325.8 ± 19.7	101.9 ± 8.2

[a] Results are clarified as average value ± standard deviation

[b] Energy dissipation before breaking, as calculated by the area under the stress−strain curves